

Rapid Oscillations in Cataclysmic Variables. XVII. 1RXS J070407+262501

Joseph Patterson¹, John R. Thorstensen², Holly A. Sheets^{2,3}, Jonathan Kemp^{4,1}, Laura Vican¹, Helena Uthas⁵, David Boyd⁶, Michael Potter⁷, Tom Krajci⁸, Tut Campbell⁹, George Roberts¹⁰, Donn Starkey¹¹, and Bill Goff¹²

ABSTRACT

We present a study of the recently discovered intermediate polar 1RXS J070407+262501, distinctive for its large-amplitude pulsed signal at $P = 480$ s. Radial velocities indicate an orbital period of 0.1821(2) d, and the light curves suggest 0.18208(6) d. Time-series photometry shows a precise spin period of 480.6700(4) s, decreasing at a rate of 0.096(9) ms yr⁻¹, i.e. on a time scale $P/\dot{P} = 2.5 \times 10^6$ yr. The light curves also appear to show a mysterious signal at $P = 0.263$ d, which could possibly signify the presence of a “superhump” in this magnetic cataclysmic variable.

Subject headings: keywords: stars

1. Introduction

1RXS J070407+262501 (hereafter RX0704) is a weak hard X-ray source coinciding with a 16th magnitude star (USNO 1125.04825852). Gänsicke et al. (2005, hereafter G05) associated this star with the X-ray source, and described its properties: a high-excitation cataclysmic variable (CV) with an orbital period near 4 hours, and a strong optical pulse with a fundamental period of 480

¹Department of Astronomy, Columbia University, 550 West 120th Street, New York, NY 10027

²Department of Physics and Astronomy, Dartmouth College, 6127 Wilder Laboratory, Hanover, NH 03755

³Now at Department of Astronomy, University of Maryland College Park, MD 20742-2421

⁴Joint Astronomy Centre, University Park, 660 North A’ohoku Place, Hilo, HI 96720; j.kemp@jach.hawaii.edu

⁵University of Southampton, Department of Physics and Astronomy, Highfield, Southampton SO17 1BJ, UK

⁶CBA Oxford, 5 Silver Lane, West Challow, Wantage, Oxon, OX12 9TX, UK; drsboyd@dsl.pipex.com

⁷CBA Baltimore, 3206 Overland Ave, Baltimore, MD, 21214; mike@orionsound.com

⁸CBA New Mexico, PO Box 1351, Cloudcroft, NM, 88317; tom_krajci@tularosa.net

⁹CBA Arkansas, 7021 Whispering Pine Road, Harrison, AR, 72601; jmontecamp@yahoo.com

¹⁰CBA Tennessee, 2007 Cedarmon Drive, Franklin, TN, 37067; georgeroberts@comcast.net

¹¹CBA Indiana, 2507 County Road 60, Auburn, IN, 46706; donn@starkey.ws

¹²CBA Sutter Creek, 13508 Monitor Lane, Sutter Creek, CA, 95685; b-goff@sbcglobal.net

s (and most of the power at 240 s, the first harmonic). This suggests membership among the DQ Herculis stars, or “intermediate polars” as they are also called (for reviews and rosters, see Patterson 1994; Hellier 1996; Mukai 2009). This has now been confirmed by detection of X-rays pulsed with the same period (Anzolin et al. 2008), which is interpreted as the spin period of an accreting, magnetic white dwarf.

The very high pulse amplitude caught our eye; we had been looking for a star with a pulsed signal sufficiently strong that small-telescope observers could track nearly every pulse – and thereby accumulate a long and detailed observational record of the periodicity. This was partially successful, although the star is a little faint, and the pulse a little fast, to be tracked in fine detail by small telescopes. Still, we managed to learn the periods precisely, and to track long-term changes in pulse period. We report here on the results of that 2006-2010 campaign.

2. Spectroscopy

We obtained spectra, using the 1.3 m McGraw-Hill telescope at MDM Observatory, the Mark III spectrograph, a 600 line mm^{-1} grism, and a SITe 1024×1024 CCD detector. The spectra covered 4650-6980 Å with 2.3 Å pixel^{-1} and a slightly undersampled FWHM resolution of 4 Å over most of the range. The wavelength scale was established by frequent observation of arc lamps. The 2 arc-second slit produced light losses, so the flux measurements are only approximate.

We obtained a pair of 15 minute exposures on 2006 January 10, and much more extensive observations during January 18-22. Our observations span a range of 9.4 hours in hour angle, which suppressed daily cycle count ambiguities in the period determination. Table 1 contains the log of observations.

Figure 1 shows the mean spectrum. The synthetic magnitude, computed using the passband from Bessell (1990) is $V = 17.3$. Strengths of Balmer, He I, and He II emission lines are given in Table 2. Their equivalent widths are typical of novalike variables, and especially those with strong X-ray fluxes. The spectrum is fairly similar to that of G05, although our continuum flux level is nominally ~ 1 magnitude fainter. We do not detect any absorption features from a secondary star.

We measured radial velocities of the $\text{H}\alpha$ emission by convolving its profile with the derivative of a Gaussian, optimized for a line profile of 14 Å FWHM. Schneider & Young (1980) describe the line-measurement algorithm. The next strongest line, $\text{H}\beta$, also yielded some useable velocities, but with lower signal-to-noise. To search for periods, we analyzed the $\text{H}\alpha$ velocities with the “residual-gram” method described by Thorstensen et al. (1996). This yielded an unambiguous cycle count and a period of 262.2 ± 0.4 min. This is consistent with the less precise period suggested by G05. The best fit sinusoid of the form $v(t) = \gamma + K \sin[2\pi(t - T_0)/P]$ has

$$\begin{aligned} T_0 &= \text{HJD } 2,453,755.8430(29) \\ P &= 0.1821(2) \text{ d} \end{aligned} \tag{1}$$

$$\begin{aligned} K &= 191(12) \text{ km s}^{-1} \\ \gamma &= 65(9) \text{ km s}^{-1}. \end{aligned}$$

Fig. 2 shows this fit superposed on the folded H α velocities; note that T_0 is the time of blue-to-red crossing.

3. Photometry and Light Curves

We obtained time-series photometry on 43 nights, totaling 250 hours, during 2006-2010. About one-fifth consists of fast (~ 15 s resolution) integrations with CCD cameras on the 1.3 m telescope of MDM Observatory. The rest is slower (40-80 s) photometry with various 20-35 cm telescopes in the Center for Backyard Astrophysics network (CBA, Patterson 1998). About half the nights are quite long, ~ 8 hr, and some are very short (~ 1 hr, suitable only for a pulse timing). The brightness generally varied in the range $V = 16.4$ -17.2. Brightness changes up to 0.4 mag were noted on consecutive nights, but we could not detect any pattern in these changes. In this program of differential photometry, the quality of the nights was mixed: some were photometric, but many were somewhat cloudy, since we considered this star a good target for cloudy nights (because we were primarily interested in the timing of its powerful and fast pulse).

On every night and at all times, the star flashed a powerful 240 s wave in the light curve, of ~ 0.3 mag full amplitude (peak-to-trough). This is shown in the upper frame of Fig. 3. The lower frame shows the power spectrum of one night's light curve. This indicates a dominant signal at 359.5 c d^{-1} (towering off-scale at a power of 1600), an obvious signal at lower frequency, and many harmonics of the latter. This reveals the signal's underlying nature: a 480 s periodicity with a double-hump waveform and other departures from a pure sinusoid. All of this agrees with the study of G05.

On six occasions, spread over 40 nights, we obtained ~ 8 hr coverage at high time resolution with the 1.3 m telescope. On each night, we folded the data on the precise 480 s period; the resultant waveforms were identical each time. Fig. 4 shows the waveforms for the two best pairs of consecutive nights (clear throughout), demonstrating how precisely the waveform repeats. Here we have defined zero as the phase of the broader, deeper minimum – which always precedes the sharper maximum. (This is different from the more practical phase convention used below.) Although only a few nights permitted study of these subtle odd-even effects from the synchronous summations, we could carry out the study for six nights by examining the harmonics. Harmonics carry information about the waveform, and we found that *the phasing of the high harmonics was repeatable from night to night*. This indicates a repeatable waveform, at least on those six nights.

4. Detailed Period Structure and Orbital Effects

The 2006-7 campaign primarily relied on MDM time series, while in 2009-10 we had mainly CBA coverage. We analyzed these two campaigns separately.

4.1. The 2009-10 Campaign

In 2009-10 we had only small telescopes available, but obtained 8 consecutive long nights of coverage from several terrestrial longitudes. This overcame all problems of aliasing. The upper frame of Figure 5 shows the low-frequency power spectrum, with significant signals flagged with their frequency in cycles d^{-1} (± 0.015). The 5.479 c d^{-1} signal is apparently the orbital frequency, and the 3.805 c d^{-1} signal is some unknown longer-period wave (discussed in Sec. 7 below). Inset is the power-spectrum window, which demonstrates that there are no ambiguities from aliasing. The middle frame shows the waveforms of these two signals, with an arbitrary zero-point (see caption). The bottom frame shows other segments of the 8-night power spectrum. Note that the immediate vicinities of the two strong signals at ω_{spin} and $2\omega_{\text{spin}}$ show the same picket-fence pattern as the spectral window in the upper frame. This indicates no significant aliasing, and no systematic amplitude or frequency modulation. There is a small but significant peak red-shifted by $5.477 \pm 0.015 \text{ c d}^{-1}$ from ω_{spin} . This is apparently the $\omega_{\text{spin}} - \omega_{\text{orb}}$ feature, a common syndrome in DQ Her stars, probably arising from the reprocessing of pulsed flux in structures fixed in the orbital frame (analogous to the sidereal/synodic lunar month).

4.2. The 2006-7 Campaign

In 2006-7 most of the coverage was with the MDM telescope, and consisted of two 9-night clusters with a total span of 48 nights. Each cluster was somewhat sparse due to intervening bad weather, and there were no data from distant longitudes. The result was data of high signal-to-noise and good definition of the periodic signals – but fairly poor rejection of aliases. This nicely complemented the strengths of the 2009-10 campaign.

The light curves and power spectra were very similar to those of 2009-10. In addition to the obvious powerful signals, a signal was sometimes manifest near $5\text{--}6 \text{ c d}^{-1}$, and the lower orbital sideband of the spin frequency near 174.25 c d^{-1} . The latter provided some additional and accurate measures of ω_{orb} (assuming that the observed sideband of the spin frequency is always separated by exactly ω_{orb}). These are listed in Table 3. The overall result, averaging over these estimates, is $\omega_{\text{orb}} = 5.492(2) \text{ c d}^{-1}$, or $P_{\text{orb}} = 0.18208(6) \text{ d}$.

This orbital period, mainly based on a 48-night baseline, is not quite accurate enough to establish a unique cycle count during the 3-year gap between campaigns. However, one consecutive-night pair in 2008-9 yielded a candidate detection of the orbital signal. With a likely orbital maximum

light at HJD 2454850.619, only one alias is permitted, and the (candidate) orbital ephemeris becomes

$$\text{Orbital maximum} = 2454061.966(6) + 0.182052(3)E.$$

The upper frame of Fig. 6 shows a 9-hour light curve, from which the fast periodic wave (including harmonics) has been removed¹. A possible 5-6 hour wave is present, although the 2006-7 sampling was too sparse to permit a reliable parsing into distinct periodic components at low frequency.

Superior signal-to-noise and time resolution in 2006-7 permitted closer study of the fast signals. Two consecutive nights with 8-hour light curves gave the best determination. The lower frame of Figure 6 shows the power spectrum after removal of the 480 s signal and all its harmonics. Significant signals are marked with their frequency in cycles d⁻¹ (± 0.08), and each is a harmonic of 174.27 ± 0.06 c d⁻¹. The inset frame shows the mean light curve at this frequency, which is $\omega_{\text{spin}} - \omega_{\text{orb}}$.

5. Pulse Ephemeris and Long-Term Period Change

Our campaign also had coverage distributed over each observing season, and hence is well suited for the study of long-term timing effects, since an exact cycle count can be associated with each pulse. Table 4 contains the period derived for each observing season, along with the estimate of G05 for the earlier 2004-5 season. Basically, each season is consistent with $P = 480.6700(2)$ s, except for the first season, which is puzzling (see also the $O - C$ analysis below).

This period is easily accurate enough to count cycles from one year to the next, and in Table 5 we list the times of maximum light derived for each night. Since the vast majority of the power occurs at the 240 s first harmonic, we fit each light curve with that period, and extract the time of maximum light. (Although we have cited evidence above that the odd-even asymmetry is persistent, it is only provable on the best nights, so a safer procedure is to use the powerful first harmonic.)

Figure 7 shows an $O - C$ diagram of these timings relative to a test period of 240.335031 s. The 48 points are fit by a simple parabola with an RMS residual of 0.03 cycles ($= 8$ s), within measurement error. The best fit corresponds to

$$\text{HJD pulse maximum} = 2454779.89661(3) + 0.0027816553(4)E - 4.2(3) \times 10^{-15}E^2. \quad (2)$$

Also shown, near $E = -5 \times 10^5$, are the three timings published by G05, with cycle counts E assigned to most closely match our ephemeris. These are hard to understand in view of the orderly behavior during 2006-2010. Because of the very large scatter and odd period (see Table 4), we

¹ Without this removal, slow variations are difficult to see – masked by the enormous strength of the pulsed signal.

exclude these points in the fit. The parabolic term corresponds to $dP/dt = -0.095 \text{ ms yr}^{-1}$, or a period decrease on a timescale $P/\dot{P} = 2.5 \times 10^6 \text{ yr}$.

It is evident – and fascinating – that the reprocessed signal is dominated by the fundamental, while the spin signal is obviously dominated by the first harmonic. The spin signal likely originates from gas falling radially onto the white dwarf, and the strong harmonic presumably signifies a two-pole accretor, with both poles in plain sight. But in this noneclipsing star, structures fixed in the orbital frame may see the two poles asymmetrically (from our viewing angle, which will always favor one side of the secondary, hot spot, accretion disk, etc.) That may well be the basic explanation. Fast spectroscopy of the emission lines may provide an absolute phasing of the accretion funnel’s location with the photometric pulse, as done for AO Psc by Hellier et al. (1991).

6. Comparison with X-rays

With a long-term spin ephemeris, we can compare the optical and X-ray pulsed signals. The X-ray waveform is complex, but distinguished by a fairly sharp dip in soft X-rays, presumably arising from photoelectric absorption in the accretion column. Anzolin et al. (2008) report two epochs for the absorption dip in 2006-7, which are separated, according to our ephemeris, by 30635.01 ± 0.05 cycles (of the 480 s period). So the dip location appears to be stable in phase. During 2006-7, the ephemeris for the broad minimum shown in Figure 5 is

$$\text{Broad minimum} = \text{HJD } 2454108.64254 + 0.005563318E,$$

which implies that both X-ray absorption dips (each being an average over ~ 50 spin cycles) occurred at spin phase 0.88 on the convention of Fig. 4. We could probably have concocted some explanation for simple fractions like 0.50, 0.00, and even 0.75. But 0.88 is just too challenging. As usual with DQ Her stars, the comparison of optical and X-ray phases – though precise – is mysterious.

7. The 6.3 Hour Signal

A puzzling feature of the low-frequency power spectrum in Figure 5 is the 3.8 c d^{-1} ($= 6.3 \text{ hr}$) signal. Its amplitude is similar to that of the (obviously real) orbital signal, and the inset power-spectrum window shows that it is not aliased to the orbital signal. Nor does it occur at any suspicious frequency – e.g. $1/2/3 \text{ c d}^{-1}$, which can be artifacts of differential extinction. Thus it is likely to be a real signal which maintained some coherence over the 8-night interval.

Cataclysmic variables are well-equipped to produce signals at ω_{orb} , due to eclipses, presentation effects of the orbiting secondary, an emitting hot spot, and an absorbing hot spot. But distinct signals at a nearby frequency are difficult to understand. The only such phenomenon which is (moderately) understood is the “superhump” - which probably arises from a periodic modulation of accretion-disk light induced by the secondary’s perturbation at the disk’s 3:1 resonance (e.g.,

Whitehurst & King 1991; Smith et al. 2007). About a hundred stars are known to show superhumps, and about twenty papers have explored the theory underlying the phenomenon. But no confirmed superhumpers are known to be magnetic, and no theory has allowed for that possibility. Yet in the case of RX0704, the rapid X-ray/optical pulse certifies strong magnetism, *and* disruption of the disk by that magnetism (in order to provide a radial plunge to the white-dwarf surface). Is it possible that such a star can also show superhumps?

Yes, perhaps. Retter et al. (2001, 2003) reported a 6.3 hr photometric signal in the 5.5 hr binary TV Columbae, which is also a DQ Her star. Retter et al. considered this to be a superhump, although this has not been widely accepted, because other observations of comparable sensitivity failed to show the signal (and perhaps because there was no precedent among magnetic CVs). However, it’s common among confirmed superhumpers that the signal can be somewhat transient – present and powerful in one long observing campaign, and missing in another.

But the case in RX0704 is still doubtful. This is just one weak detection – and, for that matter, a detection over just one week (8 nights). Even though it is not a simple alias, a weak signal at low frequency can potentially be produced by amplitude modulations of the orbital signal, or by more complex artifacts of the data-taking – e.g., arising from an interaction of differential extinction with the “hand-off” between different telescopes in this multi-longitude campaign. Such worries can be mitigated by a much longer observing campaign, or by the star’s decision to flash a signal of greater amplitude.

8. Summary

1. From radial velocities and photometry, we establish a precise binary period of 0.18208(5) d. This period is also manifest as a weak photometric signal, and as the lower orbital sideband ($\omega_{\text{spin}} - \omega_{\text{orb}}$) of the main pulse frequency, probably indicating a component reprocessed in structures fixed in the orbital frame.

2. The white dwarf spins with $P = 480.6700$ s, with most power at the first harmonic, very likely signifying a two-pole accretor. Oddly, the signal at the lower orbital sideband frequency (“reprocessed component”) appears to be dominated by the fundamental.

3. The X-ray dip occurs 0.12 cycles before the broader optical minimum.

4. The spin period decreases on a timescale of $P/\dot{P} = 2.5 \times 10^6$ yr.

5. There may be a low-frequency photometric signal at $P = 6.3$ hours. Future observation should seek to clarify whether this is a common feature of the star. If confirmed, this periodic wave might be a long-period manifestation of a “superhump”, with the additional novelty that it occurs in a magnetic cataclysmic variable. Further theoretical exploration of this possibility is very desirable.

We gratefully acknowledge support from the National Science Foundation (through AST-0908363 at Columbia, and grants AST-0307413 and AST-0708810 at Dartmouth), NASA grant GO11621.03a, and the Mount Cuba Observatory Foundation.

Facilities: McGraw-Hill

REFERENCES

- Anzolin, G., de Martino, D., Bonnet-Bidaud, J.-M., Mouchet, M., Gansicke, B.T., Matt, G., & Mukai, K. 2008, *A&A*, 489, 1243
- Bessell, M.S. 1990, *PASP*, 162, 1181
- Gänsicke, B.T. et al. 2005, *MNRAS*, 361, 141 (G05)
- Hellier, C. 1996, *Cataclysmic Variables: How and Why They Vary*, Cambridge Univ. Press.
- Hellier, C., Cropper, M., & Mason, K. O. 1991, *MNRAS*, 248, 233
- Mukai, K. 2009, <http://asd.gsfc.nasa.gov/Koji.Mukai/iphome/iphome.html>
- Patterson, J. 1994, *PASP*, 106, 209
- Patterson, J. 1998, *Sky and Telescope*, 96, 77
- Retter, A., Hellier, C., Augusteijn, T., & Naylor, T. 2001, *ASP Conf. Ser.* 229, 391
- Retter, A. et al. 2003, *MNRAS*, 340, 679
- Schneider, D. & Young, P.J. 1980, *ApJ*, 238, 946
- Smith, A.J., Haswell, C.A., Murray, J.R., Truss, M.R., & Foulkes, S.B. 2007, *MNRAS*, 378, 785
- Thorstensen, J.R., Patterson, J., Shambrook, A.A., & Thomas, G. 1996, *PASP*, 108, 73
- Whitehurst, R., & King, A. 1991, *MNRAS*, 249, 25

Table 1. Radial Velocities and Hour Angles

Time ^a	V (H α) (km s ⁻¹)	σ_V (km s ⁻¹)	V (H β) (km s ⁻¹)	σ_V (km s ⁻¹)	HA ^b (hh:mm)
53745.9704	-38	40	-108	60	+3:58
53745.9875	-97	42	-45	102	+4:22
53753.8997	180	21	69	72	+2:47
53753.9082	199	23	+3:00
53753.9167	157	22	208	51	+3:12
53753.9253	84	31	143	69	+3:24
53753.9338	74	19	185	41	+3:36
53753.9443	12	32	-1	39	+3:52
53753.9528	-59	30	9	86	+4:04
53753.9613	-30	44	102	43	+4:16
53753.9698	-91	25	75	193	+4:28
53753.9784	-64	36	-36	87	+4:41
53754.7713	175	19	215	144	-0:14
53754.7819	254	25	227	53	+0:01
53754.7904	291	21	+0:13
53754.7990	254	25	+0:26
53754.8075	225	35	289	100	+0:38
53754.8160	126	51	377	137	+0:50
53755.9046	56	64	135	106	+3:02
53755.9131	104	66	182	109	+3:15
53755.9216	-8	57	59	118	+3:27
53755.9408	31	48	-10	210	+3:55
53755.9493	-62	64	41	124	+4:07
53755.9578	-204	82	-20	60	+4:19
53755.9776	-250	47	-48	122	+4:48
53755.9867	-96	99	36	68	+5:01
53756.9172	-54	29	83	49	+3:24
53756.9257	24	22	123	62	+3:37
53756.9342	41	26	56	49	+3:49
53756.9427	43	24	67	74	+4:01
53756.9532	139	20	197	46	+4:16

Table 1—Continued

Time ^a	V (H α) (km s ⁻¹)	σ_V (km s ⁻¹)	V (H β) (km s ⁻¹)	σ_V (km s ⁻¹)	HA ^b (hh:mm)
53756.9617	217	15	311	51	+4:29
53756.9702	270	17	325	73	+4:41
53756.9787	277	24	316	41	+4:53
53756.9872	224	22	248	54	+5:06
53757.5922	-111	30	-32	50	-4:21
53757.6007	-23	42	-143	132	-4:09
53757.6093	-210	36	-256	88	-3:56
53757.6178	-55	33	37	129	-3:44
53757.6263	-130	28	7	79	-3:32
53757.6433	-61	24	48	204	-3:07
53757.6518	-26	29	-39	54	-2:55
53757.6603	29	26	140	69	-2:43
53757.6688	58	24	42	57	-2:30
53757.6773	192	28	129	54	-2:18
53757.6887	242	22	208	78	-2:02
53757.6972	263	19	235	88	-1:49
53757.7058	292	16	353	34	-1:37

^aHeliocentric Julian date of mid-integration, minus 2400000. Integrations were 720 and 900 s, and the time system is UTC.

^bHour angle at mid-integration.

Table 2. Spectral Features in Quiescence

Feature	E.W. ^a (Å)	Flux (10^{-16} erg cm $^{-2}$ s $^{-1}$)	FWHM ^b (Å)
HeII λ 4686	10	55	17
H β	12	61	18
HeI λ 4921	1	6	17
HeI λ 5015	1	5	20
HeII λ 5411	3	14	26
HeI λ 5876	3	13	18
H α	26	88	20
HeI λ 6678	3	9	24

^aEmission equivalent widths are counted as positive.

^bFrom Gaussian fits.

Table 3. Accurate Estimates of the Orbital Frequency

Source	Frequency [c d $^{-1}$]
Radial velocities	5.492(7)
2007a	5.495(14)
2007a (sideband)	5.495(13)
2007b	5.487(12)
2007b (sideband)	5.490(13)
2007a+b	5.494(4)
2007a+b (sideband)	5.492(3)
2010	5.479(20)
2010 (sideband)	5.477(20)
ALL	5.492(2)

Table 4. Yearly Estimates of the Pulse Period

Season	P [s]	Reference
2004-5	480.7080(44)	G05
2006-7	480.6712(10)	this work
2007-8	480.6686(14)	this work
2008-9	480.6695(6)	this work
2009-10	480.6700(3)	this work

Table 5. Times of 240 s Maximum Light

[Heliocentric Julian Days minus 2454000.]				
61.85645	63.81754	65.74801	69.82591	70.80234
100.68293	108.64128	109.75666	170.74176	179.75711
447.86435	474.95487	475.93117	779.89672	850.56729
851.56040	903.64976	904.62324	913.64979	1160.87467
1164.70780	1166.66626	1176.68833	1177.67862	1182.66893
1194.74976	1195.85697	1197.87922	1199.71220	1200.71092
1201.30060	1201.78466	1202.74428	1203.30057	1205.58990
1206.69426	1260.58046	1261.58466	1270.38303	1270.67511
1271.64317	1305.61554	1312.62812	1470.85121	1471.84707
1478.90405	1479.90545	1480.95974	1481.83037	

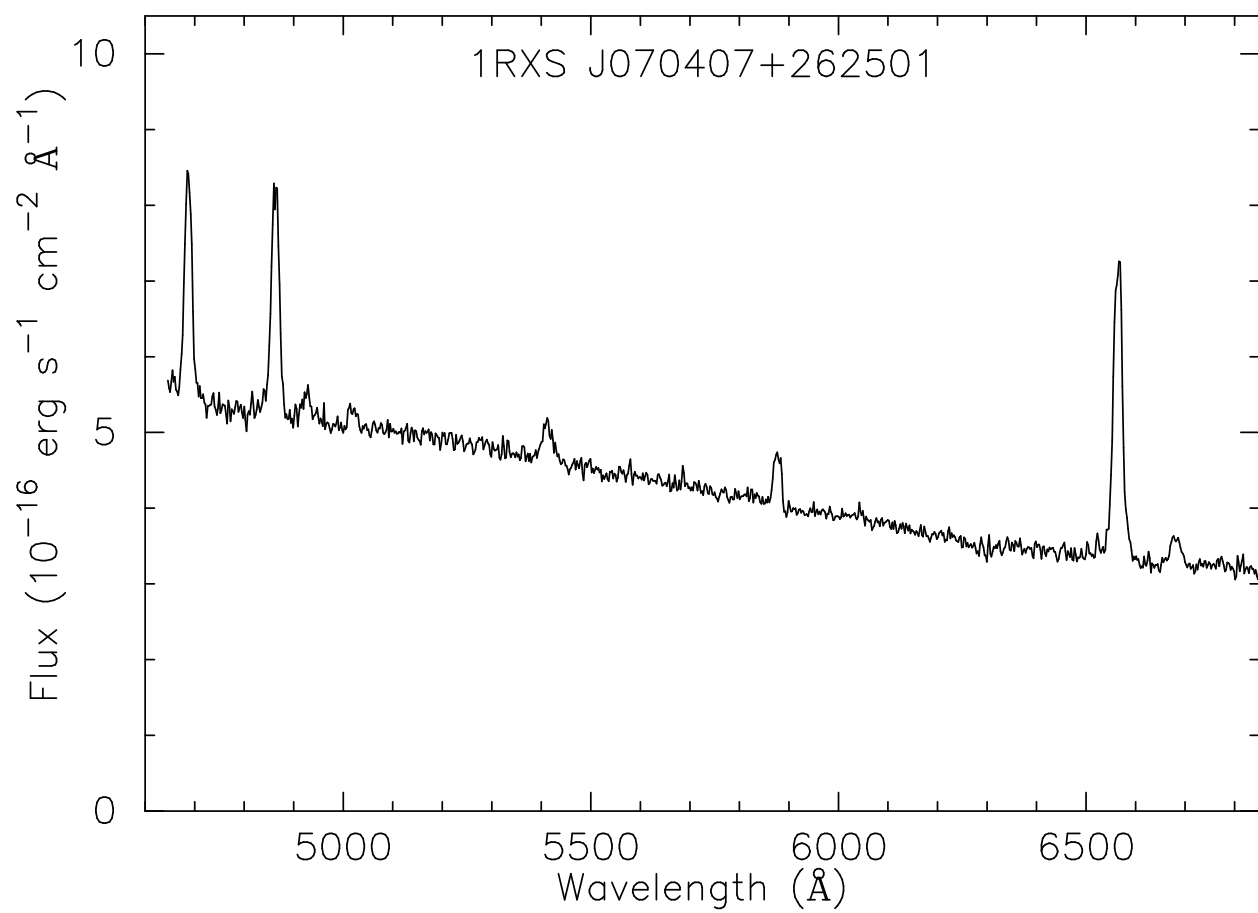


Fig. 1.— Average flux-calibrated spectrum during 2006 January. The calibration of the vertical scale is uncertain by at least 20%.

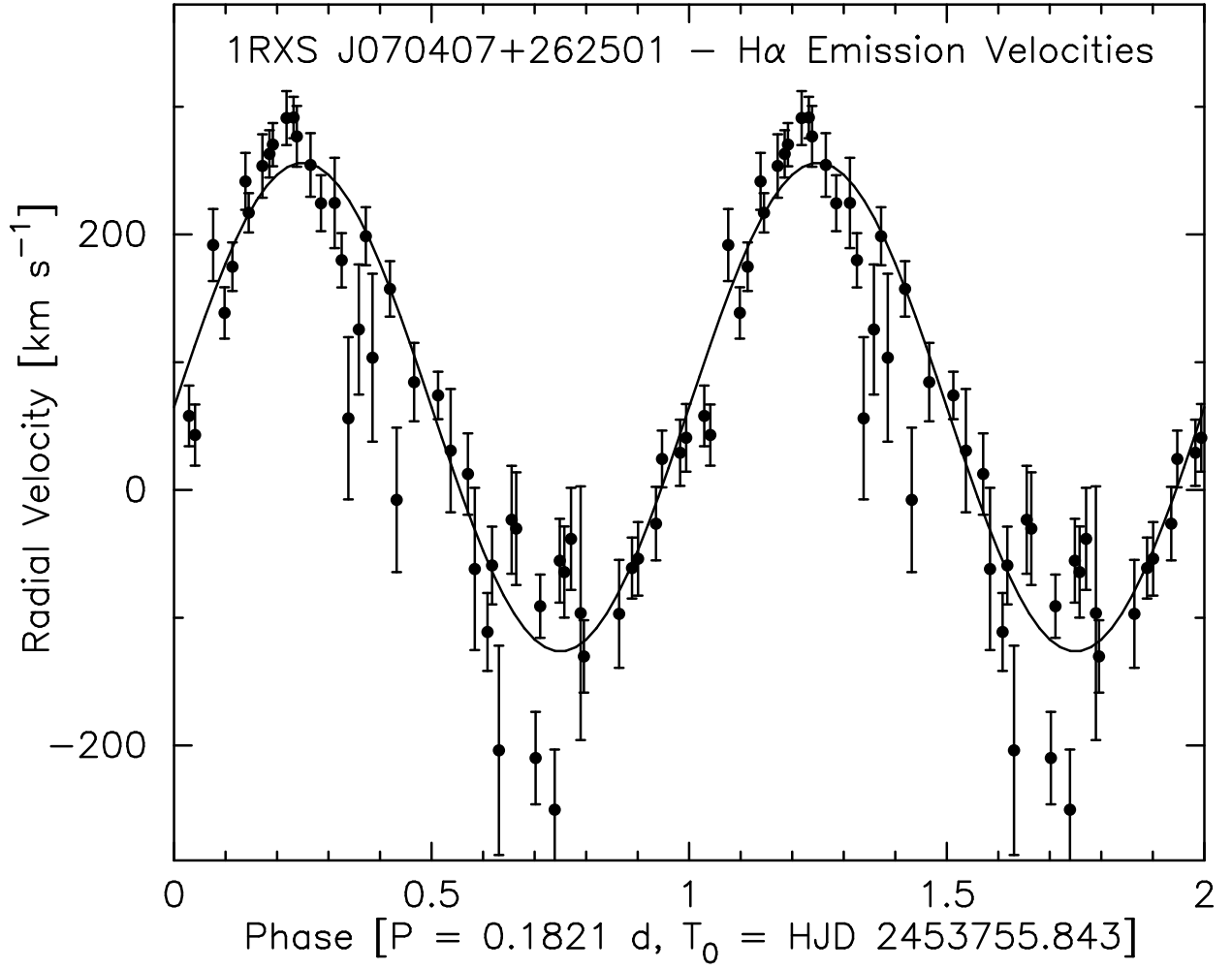


Fig. 2.— Radial velocities of the H α emission line, folded on the spectroscopic period, and with the best-fit sinusoid superposed. For continuity, all data are repeated for a second cycle. The error bars shown are 1 standard deviation, estimated from counting statistics.

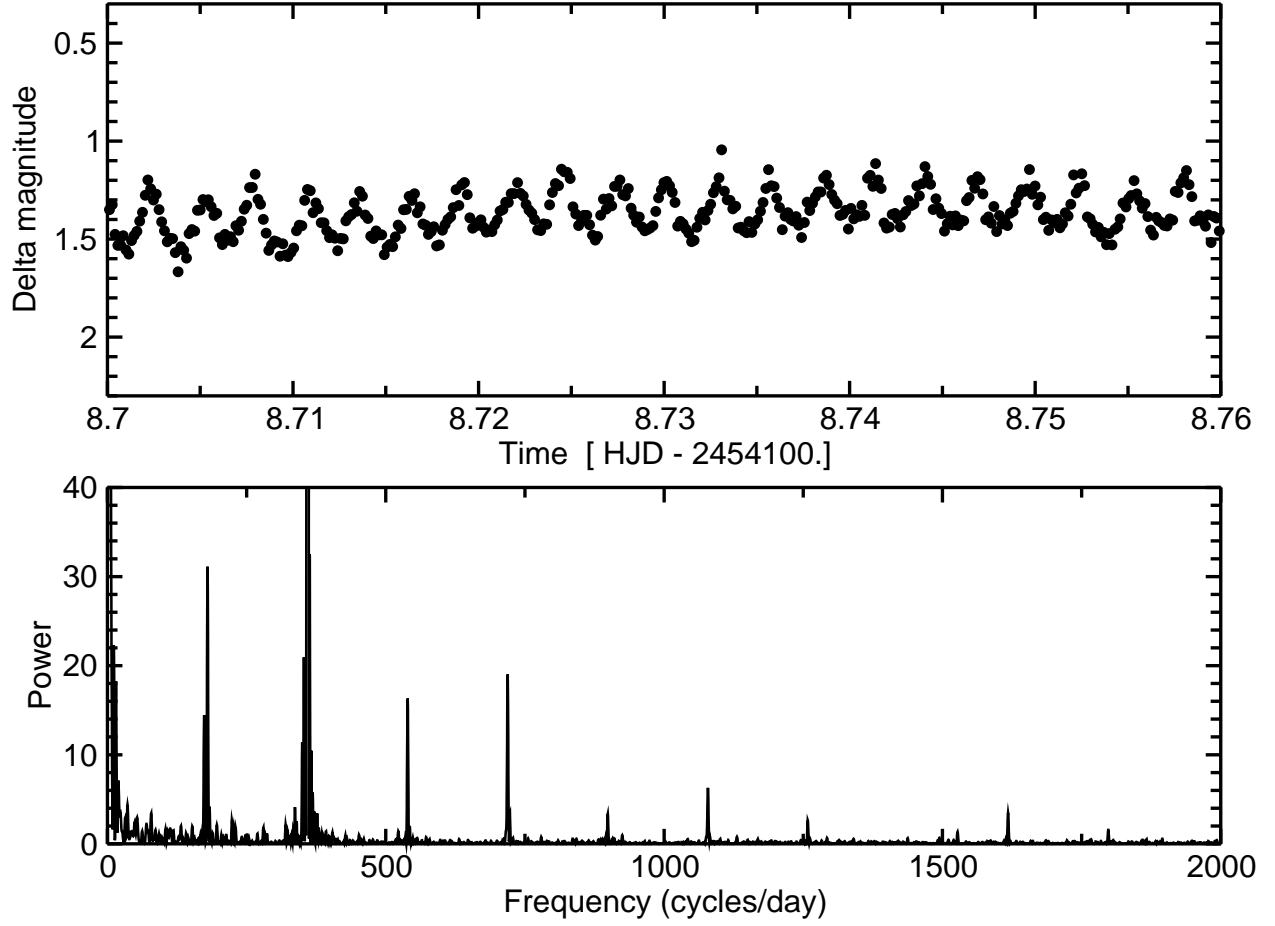


Fig. 3.— *Upper frame:* A portion of one night’s light curve, showing the large 240 s pulses. *Lower frame:* The power spectrum of the same light curve. Rising far off-scale (to a power of 1600) is the 240 s signal; other features are the 480 s fundamental and many harmonics.

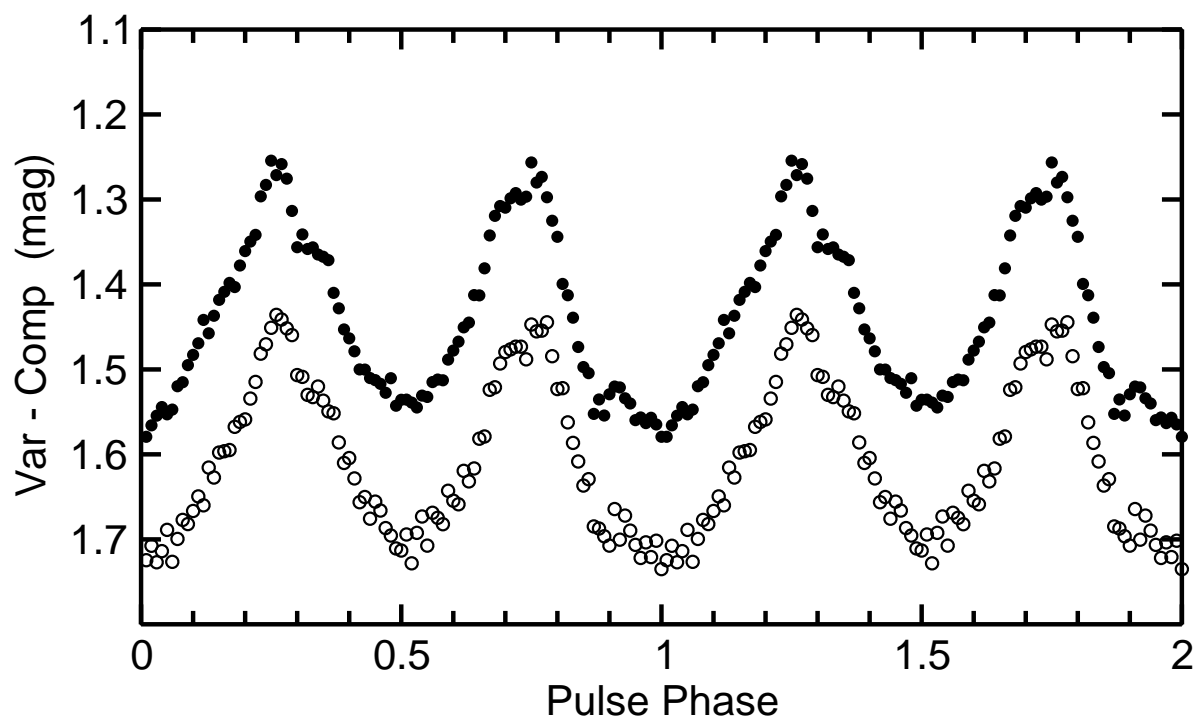


Fig. 4.— Mean light curve during two pairs of consecutive nights in 2006-7. Zero phase is defined here as the phase of the broader, deeper minimum in the 480 s cycle, and occurs at HJD 2454108.64254.

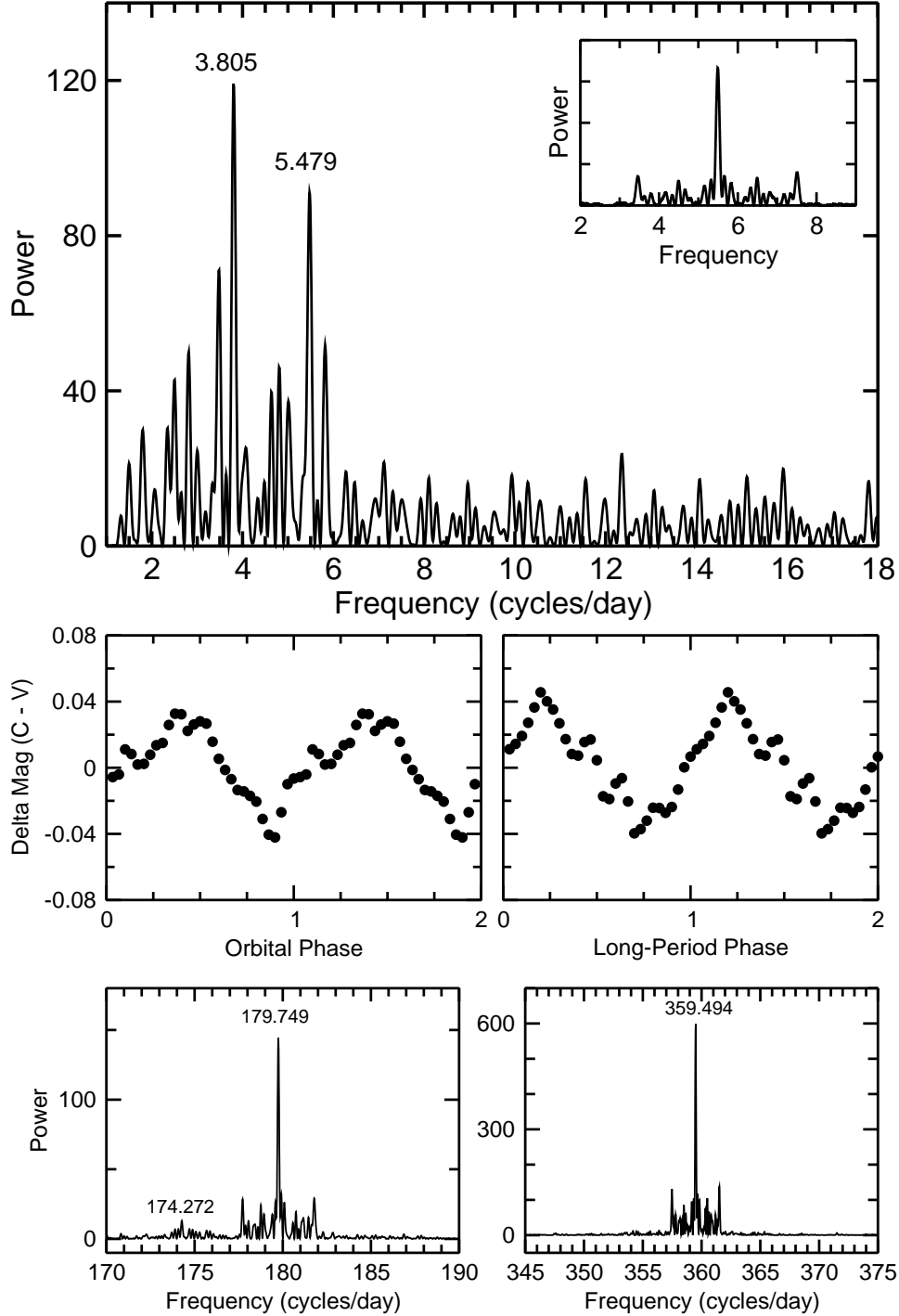


Fig. 5.— Eight-night power spectrum in 2009-10. *Upper frame:* the low-frequency region, with significant features flagged with their frequencies in cycles d^{-1} (± 0.015). Inset is the power-spectrum window of this campaign, which demonstrates that there are no problems with aliasing - and, in particular, that the peculiar signal at 3.805 c d^{-1} is not an alias. *Middle frame:* Light curves folded at these periods: each of semi-amplitude 0.04 mag. *Lowest frame:* Region near the strong signals, showing a significant peak at 174.27 c d^{-1} ($\omega_{\text{spin}} - \omega_{\text{orb}}$).

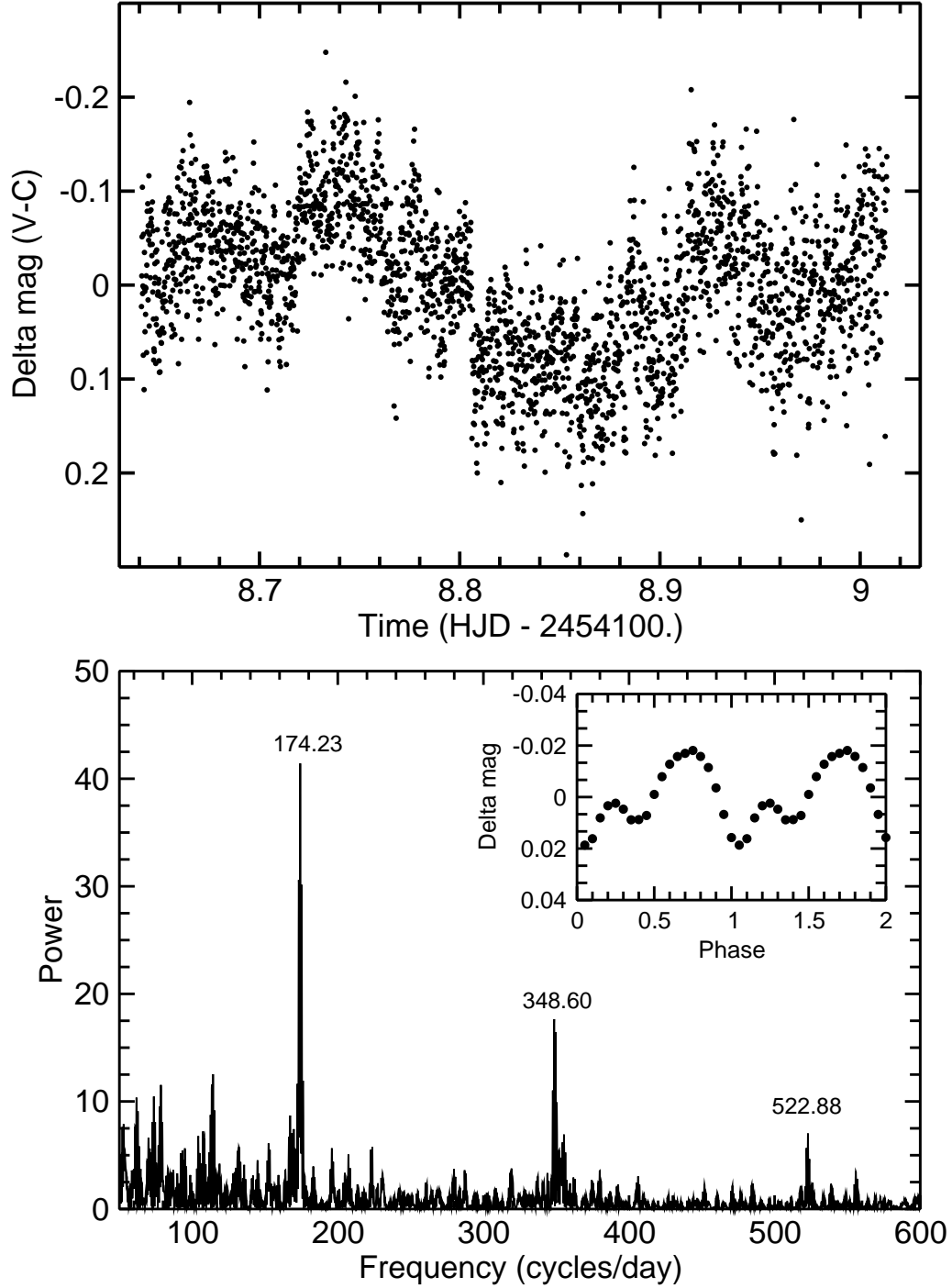


Fig. 6.— *Upper frame:* A 9-hour light curve after the rapid pulse is removed. *Lower frame:* The power spectrum of two consecutive nights after that removal. Each significant peak is labelled with its frequency (± 0.08) in cycles d^{-1} . They are integer multiples of 174.25 ± 0.05 , which we identify as $(\omega_{\text{spin}} - \omega_{\text{orb}})$. Inset is the mean waveform of that sideband signal. It is relatively weak, and is dominated by the fundamental.

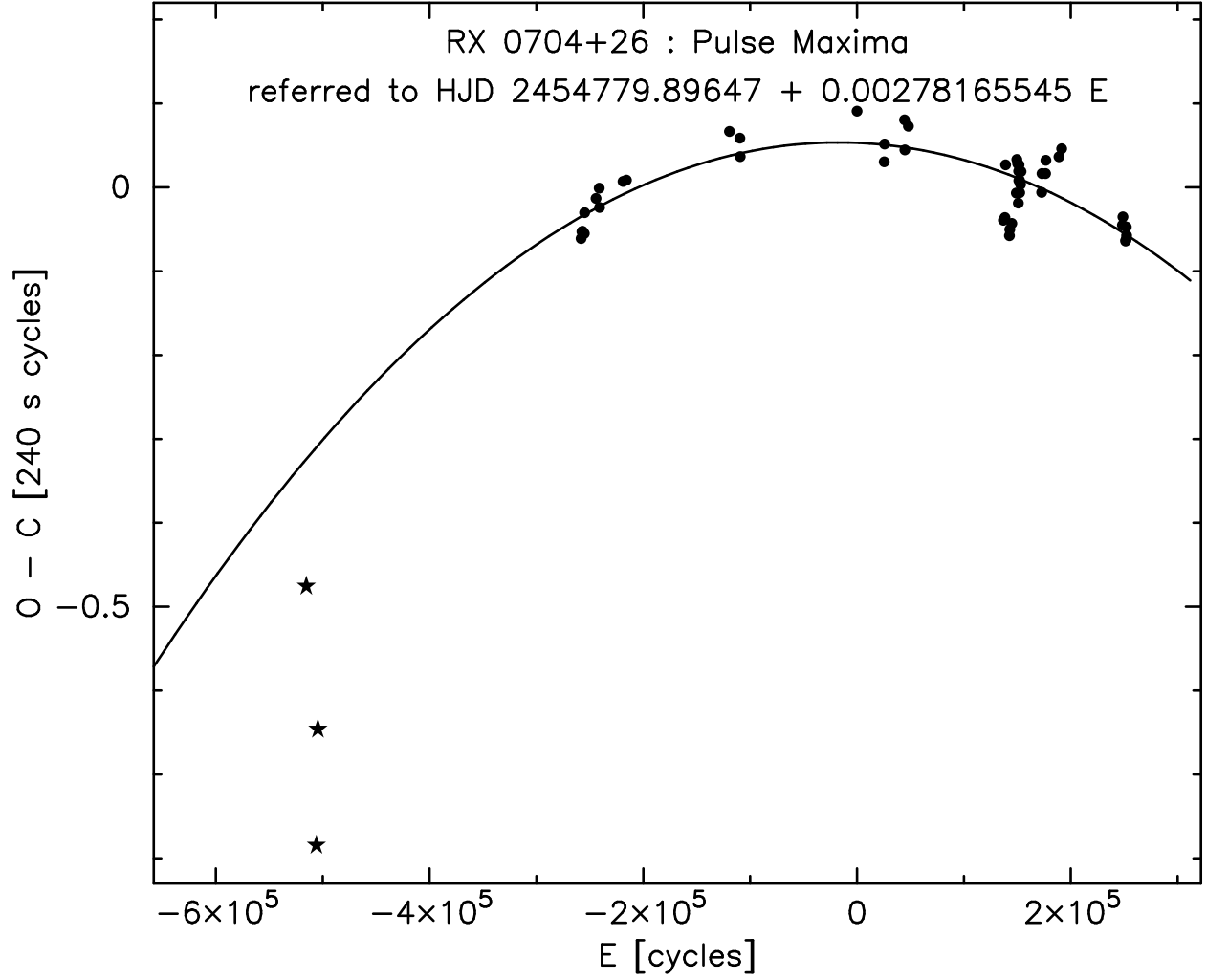


Fig. 7.— Figure 7. O-C diagram of the pulse maxima, relative to the test ephemeris HJD 2454779.89647 + 0.00278165545 E . The curve corresponds to the fitted parabola, Eq. (2). The three points near $E = -5 \times 10^5$ (stars) are those of G05; these are not included in the fit.